Atmos. Chem. Phys. Discuss., 9, 10513–10548, 2009
www.atmos-chem-phys-discuss.net/9/10513/2009/

Atmospheric Chemistry and Physics Discussions

This discussion paper is/has been under review for the journal *Atmospheric Chemistry and Physics (ACP)*. Please refer to the corresponding final paper in *ACP* if available.

Measurements of total and tropospheric ozone from IASI: comparison with correlative satellite and ozonesonde observations

A. Boynard[1,2], C. Clerbaux[1], P.-F. Coheur[3], D. Hurtmans[3], S. Turquety[1,*], M. George[1], J. Hadji-Lazaro[1], C. Keim[2], and J. Meyer-Arnek[4]

[1]UPMC Univ Paris 06, CNRS UMR 8190, Laboratoire Atmosphères, Milieux, Observation Spatiales/IPSL, Paris, France
[2]Université Paris 12 et 7, CNRS UMR 7583, Laboratoire Interuniversitaire des Systèmes Atmosphériques/IPSL, Créteil, France
[3]Spectroscopie de l'Atmosphère, Chimie quantique et Photophysique, Université Libre de Bruxelles (U.L.B.), Brussels, Belgium

[4] German Aerospace Center (DLR), German Remote Sensing Data Center (DFD), Oberpfaffenhofen, Wessling, Germany
[*] now at: UPMC Univ Paris 06, UMR 8539, Laboratoire de Météorologie Dynamique/IPSL, Paris, France

Received: 24 February 2009 – Accepted: 21 April 2009 – Published: 30 April 2009

Correspondence to: A. Boynard (anne.boynard@latmos.ipsl.fr)

Published by Copernicus Publications on behalf of the European Geosciences Union.

Abstract

In this paper, we present measurements of total and tropospheric ozone, retrieved from infrared radiance spectra recorded by the Infrared Atmospheric Sounding Interferometer (IASI), which was launched on board the MetOp-A European satellite in October 2006. We compare the IASI total ozone columns to observations from the Global Ozone Monitoring Experiment-2 (GOME-2) for one full year of observations (2008). The global distributions are in good agreement, with a correlation coefficient better than 0.9. On average, IASI ozone retrievals exhibit a positive bias compared to GOME-2 of about 4.9 DU (2.9%) to 13 DU (4.4%) depending on the season. In addition to total ozone columns, the good spectral resolution of IASI enables the retrieval of tropospheric ozone concentrations. Comparisons of IASI tropospheric columns to 490 collocated ozone soundings available from several stations around the globe have been performed for the period June 2007–August 2008. IASI tropospheric ozone columns compare well with sonde observations, with correlation coefficients of 0.95 and 0.77 for the [surface – 6 km] and [surface – 12 km] partial columns, respectively. IASI retrievals tend to overestimate the tropospheric ozone columns in comparison with ozonesonde measurements. Positive average biases of 0.15 DU (1.2%) and 3 DU (11%) are found for the [surface – 6 km] and for the [surface – 12 km] partial columns, respectively.

1 Introduction

Global monitoring of ozone (O_3) is essential since this molecule plays a key role in the photo-chemical equilibrium of the atmosphere. In the stratosphere, the ozone layer has a beneficial role as it absorbs harmful ultraviolet radiation. In contrast, ozone in the troposphere is considered by air quality agencies as one of the main air pollutants with significant impact on human health and ecosystems. In addition, ozone is one of the main greenhouse gases and plays a major role in determining the oxidizing capacity of the troposphere. For all these reasons, ozone needs to be monitored with good spatial

ACPD

9, 10513–10548, 2009

and temporal coverage in order to better understand its evolution and its impact on air quality and climate.

The measurement of tropospheric ozone is best performed by ozonesondes, which provide vertical profiles from the surface to about 30–35 km with a very high vertical resolution (~100 m) and an accuracy of about 5% in the troposphere. Soundings are performed at different locations around the globe, collected mainly in the Northern Hemisphere by the World Ozone and Ultraviolet Data Center (WOUDC). The Southern Hemisphere Additional Ozonesondes (SHADOZ) provide additional soundings in the southern and tropical regions (Thompson et al., 2004), which improve the spatial coverage of the ozonesonde network. However, the coverage remains sparse and confounds attempts to generate a complete global picture of tropospheric ozone concentrations. Despite the difficulty to separate the tropospheric ozone component from the large stratospheric contribution, satellite measurements are the best way to compliment the ozonesonde observations.

The first distributions of tropospheric ozone were obtained from ultraviolet-visible (UV-vis) measurements of the Total Ozone Measurement Spectrometer (TOMS) by subtracting stratospheric ozone from total ozone (Fishman and Larson, 1987; Fishman et al., 1990). Subsequently, several different residual-based methods have been developed to derive tropospheric ozone column from TOMS measurements (Ziemke et al., 1998; Thompson et al., 1999; Chandra et al., 2003). More recently, various approaches have been used to directly retrieve ozone profiles (and thus to derive tropospheric ozone) from the Global Ozone Monitoring Experiment (GOME) measurements (Hoogen et al., 1999b; Liu et al., 2005). UV-vis instruments remain by nature, however, weakly sensitive to the tropospheric ozone content.

Space-borne nadir-viewing instruments using the thermal infrared (TIR) spectral range to probe the troposphere offer maximum sensitivity in this layer with a vertical resolution of about 6 km (Coheur et al., 2005; Worden et al., 2007). The first distributions of total and tropospheric ozone have been retrieved from the Interferometric Monitor Greenhouse gases (IMG) instrument (Turquety et al., 2002, 2004; Coheur et al., 2005).

ACPD
9, 10513–10548, 2009

However, the instrument operated only for 10 months in 1996 on board the Japanese ADEOS platform. There are currently three nadir viewing TIR instruments providing ozone measurements from polar-orbiting satellites: the Atmospheric InfraRed Sounder (AIRS) on AQUA, the Tropospheric Emission Spectrometer (TES) on AURA and the Infrared Atmospheric Sounding Interferometer (IASI) on MetOp-A. Extended analyses, using TES and AIRS in particular have highlighted seasonal trends (Divakarla et al., 2008), enhanced pollution patterns and long-range transport (Zhang et al., 2006; Jourdain et al., 2007; Parrington et al., 2008). More recently, the enhanced capabilities of TIR sounders to probe tropospheric ozone have been used to perform an analysis of the photochemical pollution events that occurred during the 2007 summer heat wave in Southern Europe, with the recently launched IASI sounder (Eremenko et al., 2008). The latter study is a first step towards the use of infrared satellite observations to monitor tropospheric ozone and to improve the forecasts of air quality and climate models.

In this paper, we present the first global distributions of IASI total ozone columns, as well as IASI tropospheric ozone measured around several ozonesonde stations. The next section provides a description of the IASI ozone measurements, including the characteristics of the instrument and the different ozone products, such as total columns and vertical profiles. In Sect. 3, the IASI total and tropospheric ozone columns are compared with correlative ozone measurements, obtained by the GOME-2 instrument also on board the MetOp-A platform and by ozonesonde data. Section 4 summarizes the study and gives some outlooks.

2 IASI ozone measurements

2.1 IASI data

The IASI instrument (Clerbaux et al., 2007) is designed to measure temperature and moisture profiles with a very high accuracy for numerical weather prediction (Schlüssel

et al., 2005). It also allows the monitoring of trace gases to improve our understanding of the interactions between atmospheric chemistry, climate and pollution. It was launched on board the MetOp-A polar-orbiting satellite on 19 October 2006 and started to provide operational measurements in June 2007. IASI is a thermal infrared nadir-looking Fourier transform spectrometer that measures the Earth's surface and the atmospheric radiation over a spectral range of 645–2760 cm^{-1} with a 0.5 cm^{-1} spectral resolution (apodized). The ozone absorption band, near 9.6 μm, is presented in Fig. 1 as measured at three locations, representative of tropical (Hilo (Hawaii) in USA), mid-latitude (Madrid in Spain) and polar (Summit in Greenland) regions and characterized by different surface temperatures.

The IASI field of view is a matrix of 2×2 circular pixels, each with a diameter footprint of 12 km at nadir. IASI measures on average each location on the Earth's surface twice a day (at 09:30 and 21:30 local time), every 50 km at nadir, with an excellent horizontal coverage due to its polar orbit and its capability to scan across track over a swath width of 2200 km.

2.2 Ozone retrievals

Space-borne instruments record atmospheric spectra containing thousands of absorption or emission lines organized into bands. In the TIR spectral range, each spectrum results mainly from the radiative interaction between the Earth's thermal emission and the atmosphere. The absorption lines and trace gas concentrations are linked by a nonlinear function of the surface characteristics (emissivity, temperature), the temperature profile at the location of the observation, the atmospheric components interfering in the same spectral range (such as other trace gases, clouds and aerosols), as well as the instrumental characteristics, including the spectral resolution, the radiometric noise and the spectral response function. To retrieve information about the atmosphere, such as surface temperature or atmospheric trace gas concentrations from the measured radiances, an inversion algorithm needs to be applied.

Since 4 June 2007, global distributions of total ozone columns are systematically

ACPD
9, 10513–10548, 2009

retrieved, in a quasi near real time mode, from IASI Level 1 radiances distributed by Eumetsat through the Eumetcast dissemination system, for daytime and night time measurements, using a fast neural network approach (Turquety et al., 2004). For specific cases ozone concentration profiles in the troposphere and in the stratosphere with an associated error budget are derived using a line-by-line radiative transfer model coupled to an optimal estimation inversion scheme (Coheur et al., 2005). Diagnostic variables allowing accurate comparison with other data are also provided, in particular the averaging kernel functions $\mathbf{A}=\frac{\partial \hat{x}}{\partial x}$ characterizing the sensitivity of the retrieved state $\hat{x}$ to the true state x. The trace of $\mathbf{A}$ represents the number of independent elements contained in the measurements, known as the degrees of freedom for signal (DOFS) which gives an estimation of the vertical sensitivity of the retrievals. The maximum sensitivity is given by the peak of the averaging kernels at a given altitude and the vertical resolution of the retrieved profiles can be evaluated by the full width at half maximum of the averaging kernel functions.

Retrievals are only performed for cloud-free scenes, identified using a filter based on the estimation of brightness temperatures around 11 and 12 μm and on their comparison with the surface temperature provided by the European Centre for Medium-Range Weather Forecasts (ECMWF) analyses. A more detailed description of the cloud filter is given in Clerbaux et al. (2009). The next two sections present a description of the different ozone products obtained from the IASI measurements and used for the validation work presented in this paper.

2.2.1 Total ozone global distributions

Systematic retrievals of total ozone columns are performed using an algorithm based on neural network (NN) techniques (Turquety et al., 2004). The inputs of the NN are composed of clear-sky IASI spectra and of associated surface temperature and atmospheric temperature profiles from ECMWF analyses. For a full description of the algorithm the reader is kindly referred to Turquety et al. (2004).

Figure 2 presents an example of ozone total column distributions retrieved from IASI

daytime measurements made on 15 February 2008, averaged over a constant 1°×1° grid. Only measurements made with a scan angle below 32° on either side of the nadir are considered as the NN was not trained at larger scan angle values. This figure illustrates the capability of IASI to capture the spatial variability of the total ozone columns. Maximum columns are located at mid- and high latitudes and minimum columns are found in the tropics. On this day a remarkable feature of the total ozone columns located in the Eastern Atlantic around [35° N, −30° E] (see zone highlighted by the enclosed area) is observed by both IASI and GOME-2 (not shown). Due to a low pressure system located in the vicinity of the Canary Islands (see Fig. 3, which represents the geopotential height distribution at 200 hPa from the ECMWF analyses for that day) the tropopause height is massively decreased resulting in enhanced total ozone columns.

2.2.2 Ozone vertical profiles

Ozone vertical profiles are retrieved for specific areas, using a radiative transfer and retrieval software (Atmosphit) based on the Optimal Estimation Method (OEM) (Rodgers, 2000). This software also provides a full characterization of the retrievals in terms of vertical sensitivity and error sources, which is essential for an optimal use of satellite data. A detailed description of the method and the software can be found in Coheur et al. (2005), Wespes et al. (2007) and Clarisse et al. (2008).

As the retrieval of ozone profiles from atmospheric spectra is an ill-posed problem, one needs to constrain the inversion by additional information about the variables being retrieved. In the OEM, this constraint consists of a priori information, which is composed of an a priori mean profile ($\boldsymbol{x}_a$) and its associated variance-covariance matrix ($\mathbf{S}_a$). These are supposed to represent our knowledge of the state vector (vertical profile of ozone in our case) and its expected variability at the time and the place of the measurements. The ozone a priori profile and covariance matrix used in this work, displayed in Fig. 4a and b, respectively, are derived from a set of radiosonde measurements from all over the globe (available data during the period 2004–2008) connected to the UGAMP monthly climatology (Li and Shine, 1995) above 30–35 km. It is thus

ACPD
9, 10513–10548, 2009

representative of the global and annual ozone variability. Figure 4b shows higher variability in the upper troposphere-lower stratosphere between 8 and 22 km, and lower values in other altitude ranges. In particular near the surface this prior information only provides weak variability, e.g. of 10% at surface level.

In this work, the ozone profiles are retrieved in 2 km thick layers from the surface to 42 km. Surface temperature, water vapour (H_2O) partial columns and carbon dioxide (CO_2) total columns are simultaneously adjusted. The pressure and the temperature profiles are extracted from the ECMWF analyses and are collocated with the IASI measurements.

The most useful window to measure ozone in the TIR is around 9.6 μm, where ozone lines strongly dominate the 980–1070 cm^{-1} range. Ozone retrievals are performed in the 1025–1075 cm^{-1} spectral range, in order to minimize the computation time and avoid interferences with water vapour lines. This reduced window was shown to contain all the available information for retrieving ozone profiles from thermal radiance. The spectroscopic parameters have been extracted from the HITRAN 2004 database (Rothman et al., 2005).

The measurement covariance matrix including not only the instrumental noise but also other error sources such as the uncertainties on the temperature profiles is assumed to be diagonal with each diagonal element identical and equal to σ_e. The IASI radiometric noise has been estimated at 20 nW/(cm^2 sr cm^{-1}) in the ozone retrieval spectral range. We have no estimation for the other error sources. Optimization tests have been made to find the optimal value of σ_e. They have shown that the root mean square (RMS) of the spectral residuals (difference between the measured and the calculated spectra at the last fitting iteration) at different places and times was contained between 17 and 200 nW/(cm^2 sr cm^{-1}). A conservative value σ_e=70 nW/(cm^2 sr cm^{-1}), of about three times the radiometric noise, was selected for the retrievals on that basis. Although it might reduce the extent of information available in some cases, this conservative approach allows the study of ozone distributions at all latitudes and seasons using the same a priori $\boldsymbol{x}_a$ and $\mathbf{S}_a$ information. A summary of the main retrieval settings

ACPD
9, 10513–10548, 2009

is given in Table 1.

Figure 5 presents an example of a spectral fit and of the associated retrieved ozone profile for a case with a high total ozone column above the Eastern Atlantic area identified on Fig. 2. For that case, the retrieval provides low RMS values (see residual in Fig. 5a) and the retrieval constraint was therefore relaxed to a value of 20 nW/(cm^2 sr cm^{-1}) close to the instrumental noise in order to fully exploit the available information on the vertical ozone distribution. The vertical profile for this particular observation is characterized by a secondary ozone maximum with ozone concentrations of up to 6×10^6 molecules cm^{-3} at about 11 km altitude. This is consistent with the low pressure system shown in Fig. 3 which is likely to be responsible for the transport of stratospheric (ozone enriched) air masses into the tropopause region.

Figure 6a presents the averaging kernel functions for this specific observation. The averaging kernels are given for 6 km thick partial columns, from the surface to 24 km. The IASI sensitivity to the ozone profile is maximal in the troposphere ([surface – 12 km] column), but does not allow the separation of the two independent tropospheric components for this remote case above the ocean. This measurement, corresponding to a surface temperature of 291.4 K is characterized by a DOFS value of 3.5, which indicates that two additional columns in the upper troposphere and lower stratosphere can be retrieved independently from the tropospheric column. The thermal contrast (difference between the surface temperature and the temperature of the first atmospheric vertical layer) was calculated and a value of 2.4 K, was found, which is relatively unfavourable for tropospheric sounding in the TIR. Better information in the lower troposphere is expected in the case of high positive thermal contrast which interestingly accompanies frequent photochemical pollution events (Eremenko et al., 2008). As emphasized in other papers (Deeter et al., 2007; Clerbaux et al., 2009) DOFS numbers depend on both surface temperature and thermal contrast which in turn depend on surface type.

The associated error budget in Fig. 6b highlights the dominance of the smoothing error to the budget, with the measurement error and the errors introduced by the un-

ACPD
9, 10513–10548, 2009

certainties on the temperature profile also contributing to some extent. Error sources due to the simultaneous retrievals of surface properties (temperature and emissivity) and constituent concentrations such as H_2O and CO_2 contribute weakly and are not shown. The total error varies from 25 to 50% for each individually retrieved level of the profile. The errors are maximum around 10–15 km due to the tropopause variability. At all altitudes between 2 and 25 km however, there is an important reduction of errors compared to the a priori variability, showing the extent of information provided by the measurements.

3 Validation with available data

3.1 IASI/GOME-2 total column comparisons

The GOME-2 instrument, also placed aboard the MetOp-A platform is designed to continuously monitor the abundance, distribution and variability of ozone and associated species. GOME-2 is a UV-vis cross-track nadir viewing spectrometer covering the range from 240 to 790 nm. Its field of view may be varied in size from 5 km×40 km to 80 km×40 km (default). The maximum swath is about 1920 km providing almost daily global coverage at the equator.

Based on the successful work with the GOME/ERS-2 data processors, the German Aerospace Centre (DLR) plays a major role in the design, implementation and operation of the GOME-2 ground segment for total column products. It is a partner in the O3M-SAF (Satellite Application Facility on Ozone and Atmospheric Chemistry Monitoring), which is part of the EPS (Eumetsat Polar System) ground segment. The retrievals of total ozone columns from GOME-2 measurements are based on the GOME Data Processor (GDP) operational algorithm which is a classical DOAS-AMF fitting algorithm. More details on the algorithm can be found in Van Roozendael et al. (2006).

GOME-2 total ozone columns provided by the DLR are available in near real time since the 30 March 2007, through Eumetcast. A initial validation with one full year of

ACPD
9, 10513–10548, 2009

ground based and satellite measurements shows that GOME-2 total ozone products have already reached an excellent quality (Balis et al., 2008, Validation report, can be obtained from: http://wdc.dlr.de/sensors/gome2/).

For the validation of IASI total ozone column retrievals, IASI and GOME-2 total ozone column distributions are averaged over a constant $1^{\circ}\times1^{\circ}$ grid and compared over the whole year of 2008. As the UV-vis instrument provides daytime observations, only the IASI daytime measurements are compared. Figure 7 shows the seasonal global distributions of total ozone columns derived from the IASI NN retrievals compared to the GOME-2 data. Globally and seasonally both instruments observe similar structures for the ozone total columns as a function of latitude. As expected, maximum columns are observed at high latitudes whereas the minimum columns are generally located in the tropical regions (except for the ozone hole seasons). The annual ozone depletion over the Antarctic for the July-August-September and October-November-December periods is also well observed by both instruments. Relative differences between IASI and GOME-2 total ozone columns (Fig. 8) do not exceed 15%, with no significant latitudinal dependence. Although more efforts are obviously required to fully understand local discrepancies, it is partly attributable to the different observation modes. First the instruments have a different footprint on the ground (12 km for IASI (circular), 40×80 km for GOME-2) and are hence subject to different cloud contamination. Secondly, the observation geometry of the observation differs, which implies that different air masses are probed. Finally, the two instruments are characterized by different weighting functions and have different vertical sensitivities. GOME-2 has a maximum sensitivity in the stratosphere, while IASI presents a maximum sensitivity in the free troposphere. The largest differences are observed above regions characterized by extreme emissivities, such as icy or sandy surfaces (e.g. Sahara, Middle East, Siberia, and North America) not accounted for in the IASI near-real-time processing chain using the NN. Another plausible source of discrepancy in these areas might come from the presence of aerosols (e.g. above Western Africa for the first trimester).

A statistical comparison has been performed between the total ozone columns re-

trieved from IASI and GOME-2 separately for each season, at global scale and for five different latitude zones (Fig. 9). In Table 2 the correlation coefficient, the bias of the mean and the standard deviation (or RMS) from these comparisons are summarized. Over the globe, the agreement between the two distributions is very good, with correlation coefficients (R) ranging from 0.92 to 0.98 and an RMS error of 9.7 to 28.2 DU depending on the seasons. This comparison also highlights an overestimate of the IASI total ozone columns with respect to GOME-2 (positive bias ranging from 4.9 DU (2.9%) to 13 DU (4.4%)). On average over the year, the bias value is around 9 DU (~3%) which is in the same order of magnitude as that found by Osterman et al. (2008) for TES total ozone columns compared to OMI data. The detailed analysis undertaken for different latitude bands shows that the bias may be negative, e.g. at high latitudes. In particular, in the winter northern polar regions, comparisons between IASI and GOME-2 total ozone provide the largest bias (−44.0 DU), RMS (36.8 DU) and the lowest correlation coefficient (0.39) of all seasons. The highest correlation coefficients are found in the mid-latitude regions, with values higher than 0.9, except for the summer northern and the autumn southern mid-latitude regions where the correlation coefficients are lower.

3.2 IASI/Ozonesondes tropospheric column comparisons

To analyze the IASI tropospheric ozone columns, high vertical resolution profiles measured by the ozonesondes have been used. Ozonesonde measurements were obtained from the WOUDC, SHADOZ and the Global Monitoring Division (GMD) of NOAA's Earth System Research Laboratory archives. We selected fourteen stations representative of different latitudes, including mid-latitudes, polar and tropical regions and providing observations collocated to IASI measurements within a square of 110 km length and temporal coincidence of 12 h (Fig. 10 and Table 3). More details on the selection criteria are given in Keim et al. (2009) who report on an algorithm intercomparison of ozone retrievals from the IASI radiance data (including Atmosphit, used in the present analysis).

After retrievals, noisy spectra are filtered out with a filter based on the RMS of the

ACPD
9, 10513–10548, 2009

spectral residuals. We only keep spectra which have an RMS value lower than twice the σ_e value used to constrain the retrievals. We also only take into account sonde profiles collocated to at least four IASI profiles, which are then averaged. After selection, the validation of IASI tropospheric ozone columns is performed on a set of 490 sonde measurements and 4028 coincident clear-sky IASI observations during a period extending from June 2007 to August 2008.

The sonde measurements need to be smoothed (Rodgers and Connor, 2003) according to the averaging kernel matrix of the IASI retrievals in order to take into account the different vertical resolutions and to allow a meaningful comparison with the retrieved ozone profiles, using:

$$\boldsymbol{x}_{\text{smoothed sonde}} = \boldsymbol{x}_a + \mathbf{A}(\boldsymbol{x}_{\text{sonde}} - \boldsymbol{x}_a) \quad (1)$$

where $\boldsymbol{x}_{\text{sonde}}$ is the measured profile, and $\boldsymbol{x}_{\text{smoothed sonde}}$ is the smoothed ozonesonde profile.

As the sondes provide ozone profiles only up to about 30–35 km, ozonesonde profiles were connected to the a priori profile higher up.

An example of a comparison between a IASI retrieval and an ozonesonde profile is provided in Fig. 11a, for a IASI measurement point located near the Legionowo station in Poland. The figure demonstrates that the retrieved profile is in good agreement with the sonde one, with in particular the lower stratospheric part, initially far from the sonde, being nicely captured. For this example, the relative differences with respect to the smoothed ozonesonde measurements shown in Fig. 11b do not exceed 30% over the entire altitude range from the surface to 30 km. The figure also shows that the IASI measurement error is lower than the differences between both profiles.

A statistical validation of the IASI tropospheric columns with respect to the sondes is provided in Fig. 12. We compare separately two partial columns, corresponding to the integrated [surface – 6 km] and [surface – 12 km] layers. For this purpose, the sonde columns are smoothed by the corresponding merged averaging kernels from the IASI retrieval (Eq. 1). We see that the agreement is very satisfactory for both

ACPD
9, 10513–10548, 2009

columns with a correlation coefficient of 0.95 and 0.77 for the [surface – 6 km] and the [surface – 12 km] partial columns, respectively. The dynamical range of concentrations is well reproduced even for the lowest columns, unlike previous observations with other sounders (Coheur et al., 2005). IASI retrievals tend to overestimate the tropospheric ozone columns with respect to the sonde measurements. A slight bias of 0.15 DU (1.2%) is found for the [surface – 6 km] partial column while the [surface – 12 km] partial column shows a bias of 3 DU (11%). Comparisons between ozonesondes and TES tropospheric ozone retrievals also highlight a tendency to overestimate ozone (by 4 DU for TES v2 data) (Osterman et al., 2008). Similar results are found in Nassar et al. (2008).

4 Summary and conclusions

In this work, retrievals of total and tropospheric ozone columns from radiances measured by the IASI instrument have been performed.

Global scale distributions of total ozone columns retrieved from the IASI spectra have been obtained for more than a year of measurements. Comparisons of these global distributions with GOME-2 measurements have been performed for the year 2008 and showed an excellent agreement between both instruments, with a correlation coefficient better than 0.9 for each season at global scale. On average, a positive bias ranging from 4 to 13 DU depending on the season has been found. In Massart et al. (2009), it was also found that on average, IASI NN tends to overestimate the total ozone columns compared to columns obtained from the joined MLS and SCIAMACHY analysis.

The retrieval of ozone vertical profiles from a set of IASI spectra collocated with 490 ozonesonde measurements between June 2007 and August 2008 has also been performed. Tropospheric partial columns have been derived from ozone profiles and were compared to ozonesonde measurements. The comparisons showed that tropospheric ozone is also well measured, with a correlation of 0.95 for the [surface – 6 km] par-

ACPD
9, 10513–10548, 2009

tial column and a correlation of 0.77 for the [surface – 12 km] partial column. IASI retrievals overestimate the tropospheric ozone columns with respect to the sondes. We have found positive average biases of 0.15 DU (1.2%) and of 3 DU (11%) for the [surface – 6 km] and [surface – 12 km] partial column, respectively.

A new optimized algorithm based on the OEM is under development to allow ozone profile retrievals in near-real time. It will be an adaptation of the Fast Operational/Optimal Retrieval on Layers for IASI (FORLI) algorithm currently used for carbon monoxide (George et al., 2009; Turquety et al., 2009).

On the theoretical side, evidence that improvements in measuring tropospheric ozone could be gained by combining information from complementary observations in the UV-vis and the TIR has been obtained (Landgraf and Hasekamp, 2007; Worden et al., 2007), though this has yet to be tested. We plan to perform further validation, in particular by exploiting the possibilities of a combined IASI and GOME-2 ozone profile retrievals and by delivering improved ozone profile products based this combination. This will be carried out in the framework of the O3M-SAF. Work is also in progress to assimilate tropospheric ozone in a regional air quality model to assess the IASI potential of improving chemistry-transport model ozone fields and thus of improving air quality forecasts.

Acknowledgements. IASI has been developed and built under the responsibility of the Centre National des Etudes Spatiales (CNES, France). It is flown onboard the MetOp satellites as part of the Eumetsat Polar System. The IASI Level 1 data are distributed in near real time by Eumetsat through the Eumetcast dissemination system. The authors acknowledge the Ether French atmospheric database (http://ether.ipsl.jussieu.fr) for providing the IASI data. The GOME-2 Level 2 data were provided by the DLR through Eumetcast. The ozonesonde data used in this work were provided by the World Ozone and Ultraviolet Data Center (WOUDC), the Southern Hemisphere Additional Ozonesondes (SHADOZ) and the Global Monitoring Division (GMD) of NOAA's Earth System Research Laboratory and is publicly available (see http://www.woudc.org, http://croc.gsfc.nasa.gov/shadoz, http://www.esrl.noaa.gov/gmd). All the personnel of the agencies cited above for providing the ozonesonde data are acknowledged. A. Boynard is gratiful to the CNES and the "Agence De l'Environnement et de la Maîtrise

de l'Energie" (ADEME, France) for finacial support. The research in Belgium was funded by the "Actions de Recherche Concertées" (Communauté Française), the Fonds National de la Recherche Scientifique (FRS-FNRS F.4511.08), the Belgian State Federal Office for Scientific, Technical and Cultural Affairs and the European Space Agency (ESA-Prodex C90-327). The authors are grateful to INSU for publication support.

The publication of this article is financed by CNRS-INSU.

References

Balis, D., Koukouli, M., Loyola, D., Valks, P., and Hao, N.: O3M SAF second validation report of GOME-2 total ozone products, REF:SAF/O3M/AUTH/GOME-2VAL/RP/02, 2008.

Chandra, S., Ziemke, J. R., and Martin, R. V.: Tropospheric ozone at tropical and middle latitudes derived from TOMS/MLS residual: Comparison with a global model, J. Geophys. Res., 108, 4291, doi:10.1029/2002JD002912, 2003.

Clarisse, L., Coheur, P.-F., Prata, A. J., Hurtmans, D., Razavi, A., Phulpin, T., Hadji-Lazaro, J., and Clerbaux, C.: Tracking and quantifying volcanic SO_2 with IASI, the September 2007 eruption at Jebel at Tair, Atmos. Chem. Phys., 8, 7723–7734, 2008, http://www.atmos-chem-phys.net/8/7723/2008/.

Clerbaux, C., Hadji-Lazaro, J., Turquety, S., George, M., Coheur, P.-F., Hurtmans, D., Wespes, C., Herbin, H., Blumstein, D., Tournier, B., and Phulpin, T.: The IASI/MetOp I Mission: First Observations and Highlights of its Potential Contribution to GMES, COSPAR Inf. Bul., Vol 2007, 19–24, 2007.

Clerbaux, C., Boynard, A., Clarisse, L., George, M., Hadji-Lazaro, J., Herbin, H., Hurtmans, D., Pommier, M., Razavi, A., Turquety, S., Wespes, C., and Coheur, P.-F.: Monitoring of at-

mospheric composition using the thermal infrared IASI/MetOp sounder, Atmos. Chem. Phys. Discuss., 9, 8307–8339, 2009, http://www.atmos-chem-phys-discuss.net/9/8307/2009/.
Coheur, P.-F., Barret, B., Turquety, S., Hurtmans, D., Hadji-Lazaro, J., and Clerbaux, C.: Retrieval and characterization of ozone vertical profiles from a thermal infrared nadir sounder, J. Geophys. Res., 110, D24303, doi:10.1029/2005JD005845, 2005.
Deeter, M. N., Edwards, D. P., Gille, J. C., and Drummond, J. R.: Sensitivity of MOPITT observations to carbon monoxide in the lower troposphere, J. Geophys. Res., 112, D24306, doi:10.1029/2007JD008929, 2007.
Divakarla, M., Barnet, C., Goldberg, M., Maddy, E., Irion, F., Newchurch, M., Liu, X., Wolf, W., Flynn, L., Labow, G., Xiong, X., Wei, J., and Zhou, L.: Evaluation of Atmospheric Infrared Sounder ozone profiles and total ozone retrievals with matched ozonesonde measurements, ECMWF ozone data, and Ozone Monitoring Instrument retrievals, J. Geophys. Res., 113, D15308, doi:10.1029/2007JD009317, 2008.
Eremenko, M., Dufour, G., Foret, G., Keim, C., Orphal, J., Beekmann, M., Bergametti, G., and Flaud, J.-M.: Tropospheric ozone distributions over Europe during the heat wave in July 2007 observed from infrared nadir spectra recorded by IASI, Geophys. Res. Lett., 35, L18805, doi:10.1029/2008GL034803, 2008.
Fishman, J. and Larsen, J. C.: Distribution of total ozone and stratospheric ozone in the tropics: Implications for the distribution of tropospheric ozone, J. Geophys. Res, 92, 6627–6634, 1987.
Fishman, J., Watson, C. E., Larsen, J. C., and Logan, J. A.: Distribution of tropospheric ozone determined from satellite data, J. Geophys. Res., 95, 3599–3617, 1990.
George, M., Clerbaux, C., Hurtmans, D., Turquety, S., Coheur, P.-F., Pommier, M., Hadji-Lazaro, J., Edwards, D. P., Worden, H., Luo, M., Rinsland, C., and McMillan, W.: Carbon monoxide distributions from the IASI/METOP mission: evaluation with other space-borne remote sensors, Atmos. Chem. Phys. Discuss., 9, 9793–9822, 2009, http://www.atmos-chem-phys-discuss.net/9/9793/2009/.
Hoogen, R., Rozanov, V. V., and Burrows, J. P.: Ozone profiles from GOME satellite data: Algorithm and first validation, J. Geophys. Res., 104(D7), 8263–8280, 1999b.
Jourdain, L., Worden, H. M., Worden, J. R., Bowman, K., Li, Q., Eldering, A., Kulawik, S. S., Osterman, G., Boersma, K. F., Fisher, B., Rinsland, C. P., Beer, R., and Gunson, M.: Tropospheric vertical distribution of tropical Atlantic ozone observed by TES during the northern African biomass burning season, Geophys. Res. Lett., 34, L04810,

doi:10.1029/2006GL028284, 2007.
Keim, C., Eremenko, M., Orphal, J., Dufour, G., Flaud, J.-M., Höpfner, M., Boynard, A., Clerbaux, C., Payan, S., August, T., Coheur, P.-F., Hurtmans, D., Johnson, B., Koide, T., Lambkin, K., Schmidlin, F. J., Dier, H., Claude, H., and Kivi, R.: Tropospheric ozone from IASI: comparison of different inversion algorithms and validation with ozone sondes, Atmos. Chem. Phys. Discuss., in press, 2009.
Landgraf, J. and Hasekamp, O. P.: Retrieval of tropospheric ozone: The synergistic use of thermal infrared emission and ultraviolet reflectivity measurements from space, J. Geophys. Res., 112, D08310, doi:10.1029/2006JD008097, 2007.
Li, D. and Shine, K. P.: A 4-dimensional ozone climatology for UGAMP models, Internal Report No. 35, U.G.A.M.P., 1995.
Liu, X., Chance, K., Sioris, C. E., Spurr, R. J. D., Kurosu, T. P., Martin, R. V., and Newchurch, M. J.: Ozone profile and tropospheric ozone retrievals from the Global Ozone Monitoring Experiment: Algorithm description and validation, J. Geophys. Res., 110, D20307, doi:10.1029/2005JD006240, 2005.
Massart, S., Clerbaux, C., Cariolle, D., Piacentini, A., Turquety, S., and Hadji-Lazaro, J.: First steps towards the assimilation of IASI ozone data into the MOCAGE-PALM system, Atmos. Chem. Phys. Discuss., 9, 6691–6737, 2009, http://www.atmos-chem-phys-discuss.net/9/6691/2009/.
Nassar, R., Logan, J. A., Worden, H. M., Megretskaia, I. A., Bowman, K. W., et al.: Validation of Tropospheric Emission Spectrometer (TES) Nadir Ozone Profiles Using Ozonesonde Measurements, J. Geophys. Res., 113, D15S17, doi:10.1029/2007JD008819, 2008.
Osterman, G., Kulawik, S. S., Worden, H. M., Richards, N. A. D., Fisher, B. M., Eldering, A., Shephard, M. W., Froidevaux, L., Labow, G., Luo, M., Herman, R. L., Bowman, K. W., and Thompson, A. M.: Validation of Tropospheric Emission Spectrometer (TES) Measurements of the Total, Stratospheric and Tropospheric Column Abundance of Ozone, J. Geophys. Res., 113, D15S16, doi:10.1029/2007JD008801, 2008.
Parrington, M., Jones, D. B. A., Bowman, K. W., Horowitz, L. W., Thompson, A. M., Tarasick, D. W., and Witte, J. C.: Estimating the summertime tropospheric ozone distribution over North America through assimilation of observations from the Tropospheric Emission Spectrometer, J. Geophys. Res., 113, D18307, doi:10.1029/2007JD009341, 2008.
Rodgers, C. D.: Inverse Methods for Atmospheric Sounding : Theory and Practice, World Scientific, Series on Atmospheric, Oceanic and Planetary Physics, 2, Hackensack, N. J.,

2000.
Rodgers, C. D. and Connor, B.: Intercomparison of remote sounding instruments, J. Geophys. Res., 108(D3), 4116, doi:10.1029/2002JD002299, 2003.
Rothman, L. S., Jacquemart, D., Barbe, A., Chris Benner, D., Birk, M., Brown, L. R., Carleer, M. R., Chackerian Jr., C., Chance, K., Coudert, L. H., Dana, V., Devi, V. M., Flaud, J.-M., Gamache, R. R., Goldman, A., Hartmann, J.-M., Jucks, K. W., Maki, A. G., Mandin, J.-Y, Massie, S. T., Orphal, J., Perrin, A., Rinsland, C. P., Smith, M. A. H., Tennyson, J., Tolchenov, R. N., Toth, R. A., Vander Auwera, J., Varanasi, P., and Wagner, G.: The HITRAN 2004 molecular spectroscopic database, J. Quant. Spectrosc. Ra., 96, 139–204, 2005.
Schlüssel, P., Hultberg, T. H., Philipps, P. L., August, T., and Calbet, X.: The operational IASI Level 2 processor, Adv. Space Res., 36, 982–988, doi:10.1016/j.asr.2005.03.008, 2005.
Thompson, A. M., Dodderidge, B. G., White, J. C., Hudson, R. D., Luke, W. T., Johnson, J. E., Johnson, B. J., Oltmans, S. J., and Weller, R.: Tropical tropospheric ozone (TTO) maps from Nimbus 7 and Earth Probe TOMS by the modified-residual method: Evaluation with sondes, ENSO signals, trends from Atlantic regional time series, J. Geophys. Res., 104, 26961–26975, 1999.
Thompson, A. M., Witte, J. C., Oltmans, S. J., and Schmidlin, F. J.: Shadoz: A tropical ozonesonde-radiosonde network for the atmospheric community, B. Am. Meteorol. Soc., 85(10), 1549–1564, 2004.
Turquety, S., Hadji-Lazaro, J., and Clerbaux, C.: First satellite ozone distributions retrieved from nadir high-resolution infrared spectra, Geophys. Res. Lett., 29, 2198, doi:10.1029/2002GL016431, 2002.
Turquety, S., Hadji-Lazaro, J., Clerbaux, C., Hauglustaine, D. A., Clough, S. A., Cassé, V., Schlüssel, P., and Mégie, G.: Operational trace gas retrieval algorithm for the Infrared Atmospheric Sounding Interferometer, J. Geophys. Res., 109, D21301, doi:10.1029/2004JD004821, 2004.
Turquety, S., Hurtmans, D., Hadji-Lazaro, J., Coheur, P.-F., Clerbaux, C., Josset, D., and Tsamalis, C.: Tracking the emission and transport of pollution from wildfires using the IASI CO retrievals: analysis of the summer 2007 Greek fires, Atmos. Chem. Phys. Discuss., 9, 7413–7455, 2009, http://www.atmos-chem-phys-discuss.net/9/7413/2009/.
Van Roozendael, M., Loyola, D., Spurr, R., Balis, D., Lambert, J.-C., Livschitz, Y., Valks, P., Ruppert, T., Kenter, P., and Fayt, C.: Ten years of GOME/ERS-2 total ozone data – The new GOME data processor (GDP) version 4: 1. Algorithm description, J. Geophys. Res., 111,

D14311, doi:10.1029/2005JD006375, 2006.
Wespes, C., Hurtmans, D., Herbin, H., Barret, B., Turquety, S., Hadji-Lazaro, J., Clerbaux, C., and Coheur, P.-F.: First global distributions of nitric acid in the troposphere and the stratosphere derived from infrared satellite measurements, J. Geophys. Res., 112, D13311, doi:10.1029/2006JD008202, 2007.
Worden, H. M., Logan, J. A., Worden, J. R., Beer, R., Bowman, K., Clough, S. A., Eldering, A., Fisher, B. M., Gunson, M. R., Herman, R. L., Kulawik, S. S., Lampel, M. C., Luo, M., Megretskaia, I. A., Osterman, G. B., and Shephard, M. W.: Comparisons of Tropospheric Emission Spectrometer (TES) ozone profiles to ozonesondes: Methods and initial results, J. Geophys. Res., 112, D03309, doi:10.1029/2006JD007258, 2007.
Zhang, L., Jacob, D. J., Bowman, K. W., Logan, J. A., Turquety, S., Hudman, R. C., Qinbin, L., Beer, R., Worden, H. M., Worden, J. R., Rinsland, C. P., Kulawik, S. S., Lampel, M. C., Shephard, M. W., Fisher, B. M., Eldering, A., and Avery, M.: Ozone-CO correlations determined by the TES satellite instrument in continental outflow regions, Geophys. Res. Lett., 33, L18804, doi:10.1029/2006GL026399, 2006.
Ziemke, J. R., Chandra, S., and Bhartia, P. K.: Two new methods for deriving tropospheric column ozone from TOMS measurements: Assimilated UARS MLS/HALOE and convective-cloud differential techniques, J. Geophys. Res., 103, 22115–22127, 1998.

ACPD
9, 10513–10548, 2009

Table 1. Summary of the retrieval settings.

Spectral window	1025–1075 cm^{-1}
Spectroscopic database	HITRAN 2004
A priori ($\boldsymbol{x}_a$, $\mathbf{S}_a$)	Ozonesonde profiles from 2004 to 2008 connected to the UGAMP climatology
Pressure, Temperature profiles	ECMWF
Instrumental noise	70 $nW/(cm^2\,sr\,cm^{-1})$
Adjusted parameters	O_3, surface temperature, H_2O and CO_2

ACPD
9, 10513–10548, 2009

Table 2. Summary of the correlation, the bias and the (1σ) standard deviation (RMS) of the IASI total ozone column relative to the GOME-2 data, for each season. The bias and the standard deviation are given in Dobson units.

	Jan-Feb-Mar		Apr-May-Jun		Jul-Aug-Sep		Oct-Nov-Dec	
	Corr coef	Bias (1σ)	Corr coef	Bias (1σ)	Corr coef	Bias (1σ)	Corr coef	Bias (1σ)
All latitudes	0.92	4.9 (28.2)	0.98	13.0 (9.7)	0.95	10.3 (11.6)	0.92	8.6 (13.3)
60° N–90° N	0.39	−44.0 (36.8)	0.78	9.2 (8.5)	0.85	9.9 (4.8)	0.74	9.8 (13.9)
30° N–60° N	0.90	13.0 (19.6)	0.92	16.3 (11.3)	0.77	9.1 (12.9)	0.90	9.7 (12.4)
30° S–30° N	0.72	17.3 (9.9)	0.73	12.2 (9.3)	0.49	10.5 (12.1)	0.69	11.5 (9.8)
60° S–30° S	0.93	15.6 (4.9)	0.49	14.3 (5.4)	0.94	13.0 (6.7)	0.95	10.2 (6.5)
90° S–60° S	0.57	−1.0 (17.8)	0.69	13.8 (15.4)	0.92	7.8 (19.8)	0.91	−5.8 (20.6)

ACPD
9, 10513–10548, 2009

Table 3. Ozonesonde station locations, data providers, and the number of coincidences used for the ozone validation.

Ozonesonde Station	Latitude, °N	Longitude, °E	Data Source	Number of Sondes data
Summit (Greenland)	72.6	−38.5	GMD	37
STN221 (Legionow, Poland)	52.2	14.1	WOUDC	33
STN318 (Valentia Observatory, Ireland)	51.9	−10.2	WOUDC	43
STN156 (Payerne, Switzerland)	46.8	6.9	WOUCD	95
STN012 (Sapporo, Japan)	43.0	141.3	WOUDC	27
STN308 (Madrid/Barajas, Spain)	40.4	−3.6	WOUDC	37
Boulder (USA)	40.0	−105.2	GMD	33
Wallops Island (USA)	37.9	−75.5	WOUDC	40
STN014 (Tsukuba Tateno, Japan)	36.0	140.1	WOUDC	40
STN190 (Naha, Japan)	26.2	127.7	WOUDC	24
Hilo (Hawaii, USA)	19.4	−155.0	GMD	31
Nairobi (Kenya)	−1.3	36.8	SHADOZ	19
Java (Indonesia)	−7.6	112.6	SHADOZ	5
STN323 (Neumayer, Antarctic)	−70.7	−8.3	WOUDC	26

ACPD
9, 10513–10548, 2009

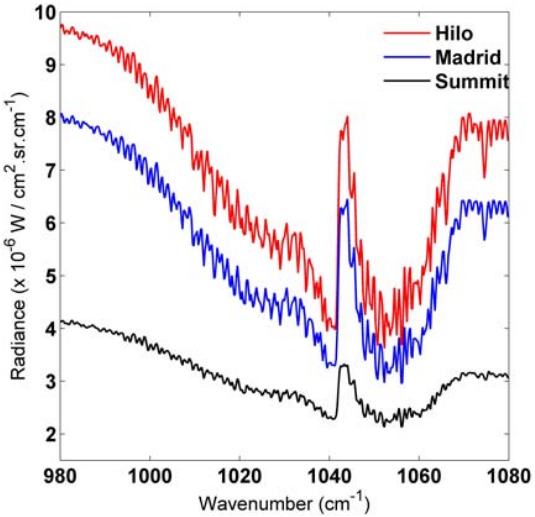

Fig. 1. Clear-sky IASI radiance spectra around the intense ozone absorption band at 9.6 μm recorded at Hilo (Hawaii) in USA (red), Madrid in Spain (blue) and Summit in Greenland (black). Spectra are characterized by surface temperatures of 299.5, 287.1 and 255.5 K, respectively.

ACPD
9, 10513–10548, 2009

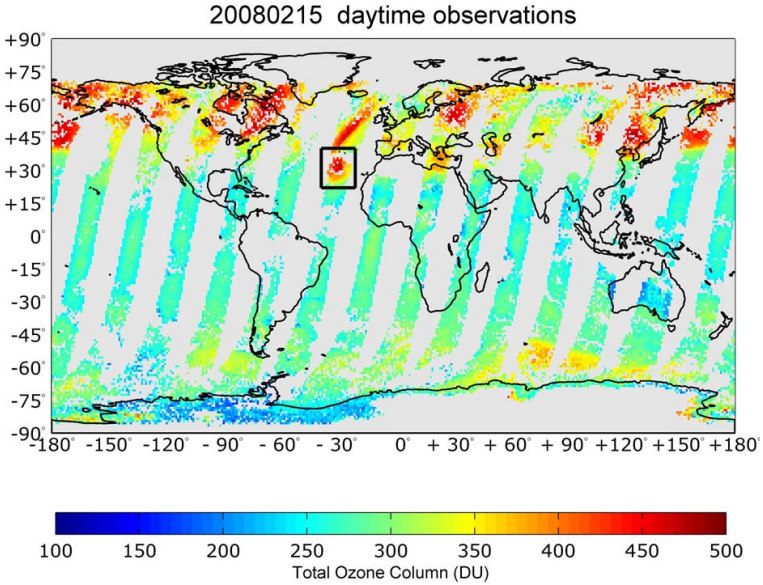

Fig. 2. Global distribution of total ozone columns obtained using the NN algorithm for daytime cloud filtered IASI observations on 15 February 2008. The data are averaged over a 1°×1° grid. Only measurements made with a scan angle below 32° on either side of the nadir are considered in the retrievals.

ACPD
9, 10513–10548, 2009

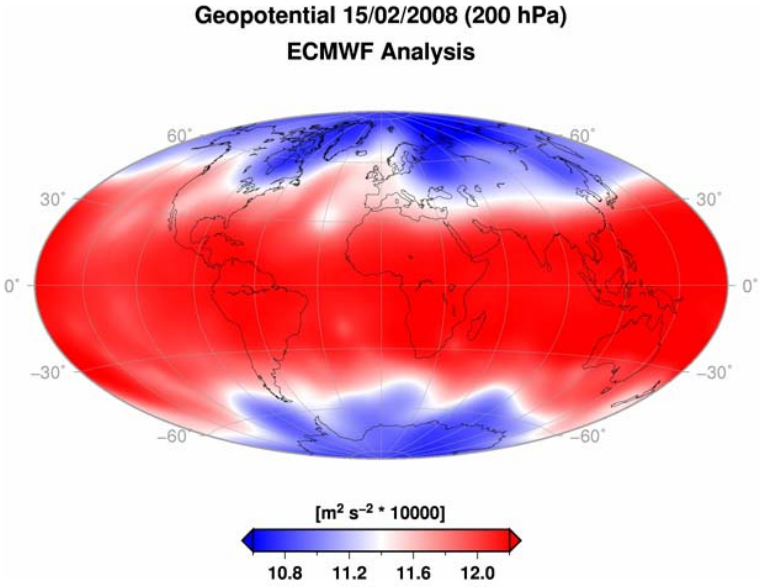

Fig. 3. Global distribution of the geopotential height at 200 hPa obtained from the ECMWF operational analyses on 15 February 2008 showing a low pressure system over the Canary Islands.

ACPD
9, 10513–10548, 2009

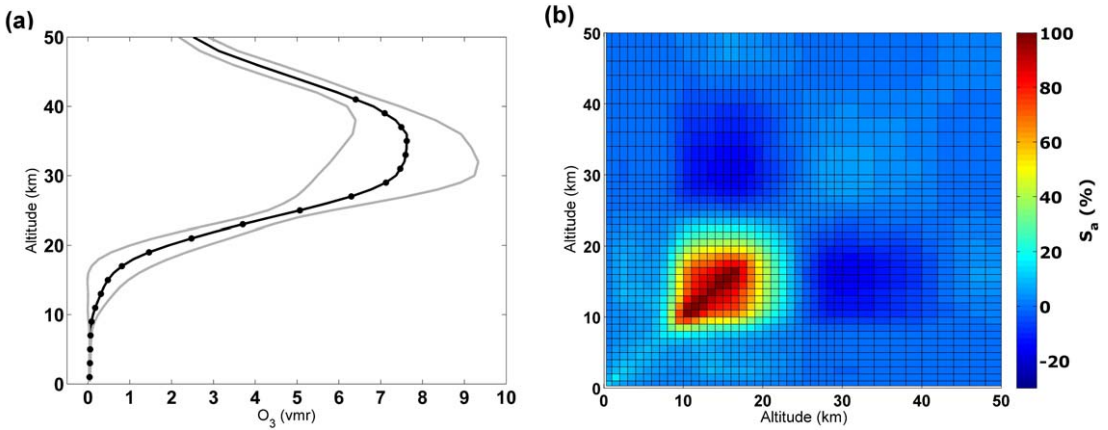

Fig. 4. (a) Global ozone a priori profile (black line) with its variability (grey lines, square root of the diagonal elements of the ozone a priori variance-covariance matrix) and the retrieval levels in black dots. **(b)** Global ozone a priori variance-covariance matrix ($\mathbf{S}_a$) in percent built from radiosonde measurements for the period 2004–2008.

ACPD
9, 10513–10548, 2009

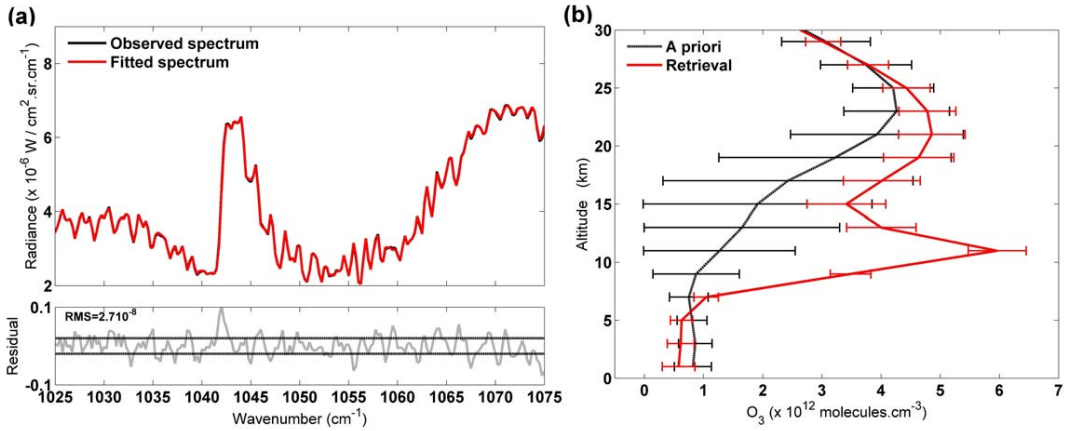

Fig. 5. (a) Spectral fit and residual for a IASI measurement made on 15 February 2008 in the Eastern Atlantic (34.8° N, −29.3° E); the black lines at ±20 nW/(cm^2 sr cm^{-1}) correspond to the IASI radiometric noise value used to constrain this retrieval. **(b)** Associated retrieved (red) as well as a priori (black) ozone profile in number density units.

ACPD
9, 10513–10548, 2009

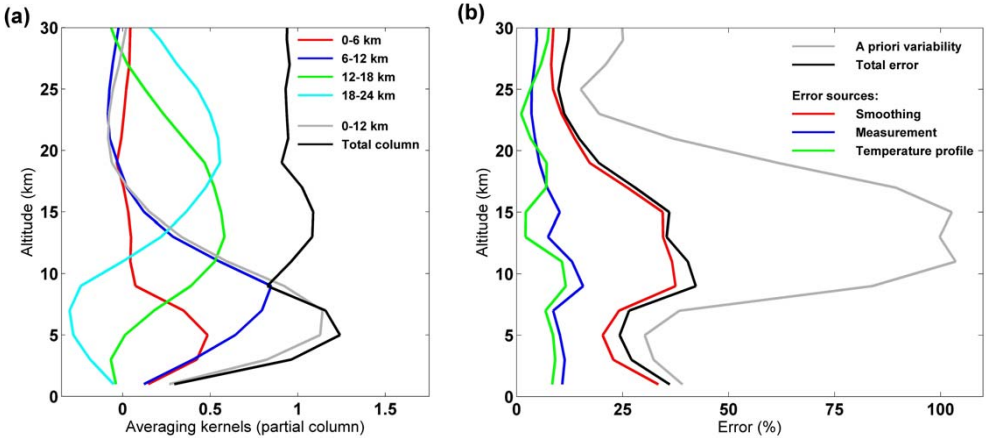

Fig. 6. **(a)** Averaging kernel functions for the [surface – 6], [6–12], [12–18], and [18–24] km partial columns characterizing the retrieval shown in Fig. 4. The averaging kernel associated with the [surface – 12] km tropospheric column is also shown. The black curve represents the integrated measurement response. **(b)** Associated error budget. The a priori variability and total errors are given by the square root of the diagonal elements of the a priori covariance matrix and the error covariance matrix, respectively. The contributions of the surface properties (surface temperature and emissivity), H_2O and CO_2 columns are not shown.

ACPD
9, 10513–10548, 2009

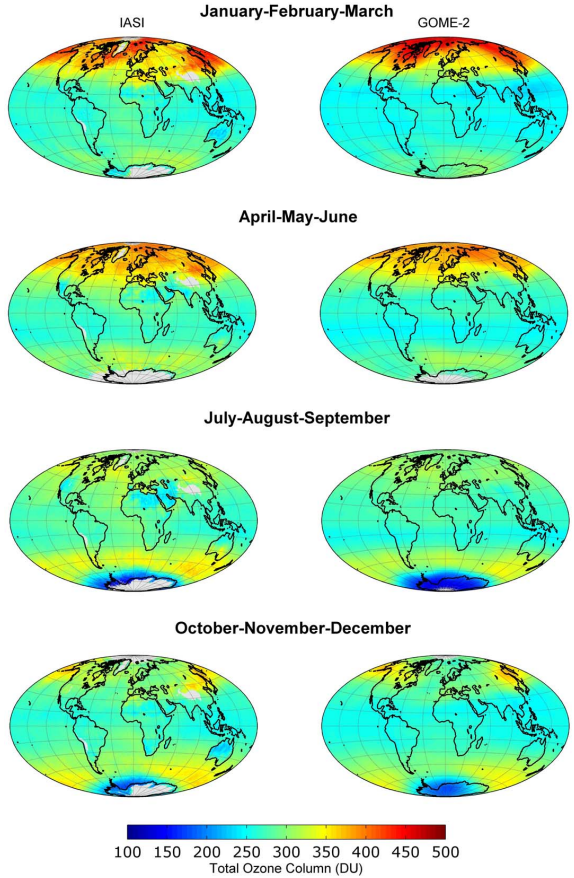

Fig. 7. Global distributions for three months averaged periods (1°×1° grid): (left) IASI total ozone columns compared to (right) GOME-2 retrieved total ozone columns for daytime measurements. On the IASI maps, grey areas correspond to data recorded over topography (altitude higher than 2 km) that have been filtered out.

ACPD
9, 10513–10548, 2009

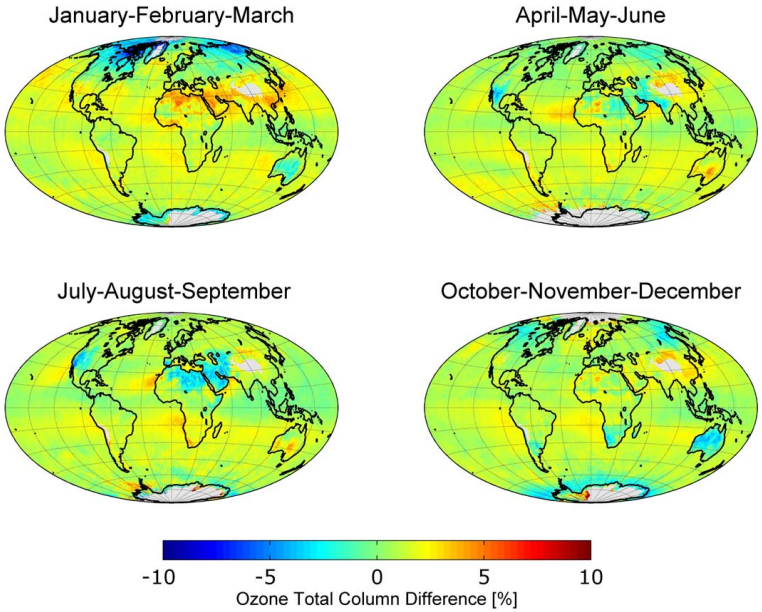

Fig. 8. Relative differences between IASI and GOME-2 total ozone columns for daytime measurements and for three month averaged periods (1°×1° grid). The relative differences are calculated according to: 100*(IASI-GOME2)/GOME2.

ACPD
9, 10513–10548, 2009

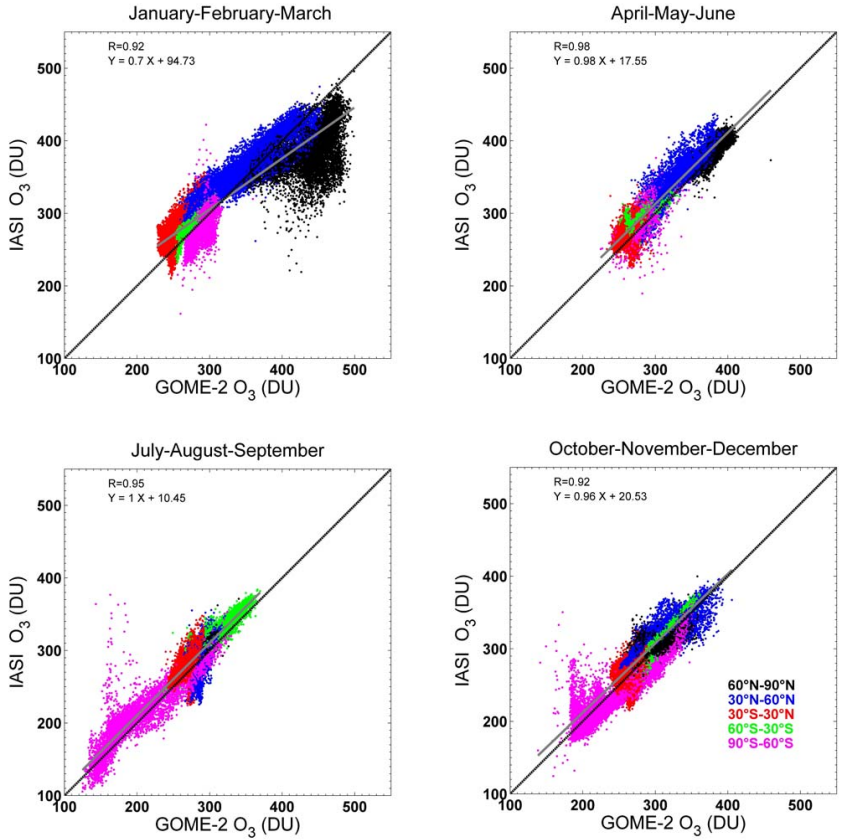

Fig. 9. Scatter plots of the IASI and GOME-2 total ozone columns for three months averaged periods (Jan-Feb-Mar, Apr-May-Jun, Jul-Aug-Sep, Oct-Nov-Dec). The plots show averaged data over a $1^{\circ} \times 1^{\circ}$ grid. The shaded line represents the linear regressions between all data points and the black line, of unity slope, is shown for reference.

ACPD
9, 10513–10548, 2009

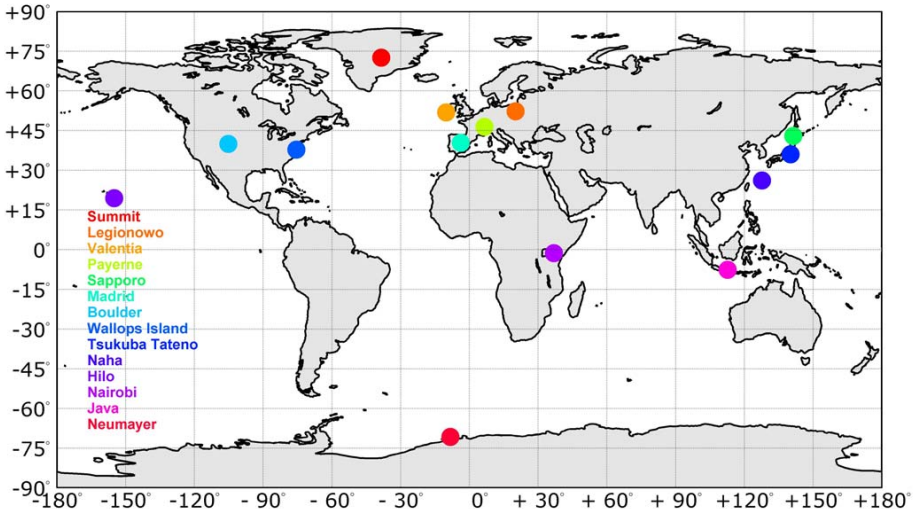

Fig. 10. Geographic locations of the fourteen ozonesonde validation stations used in this study.

ACPD
9, 10513–10548, 2009

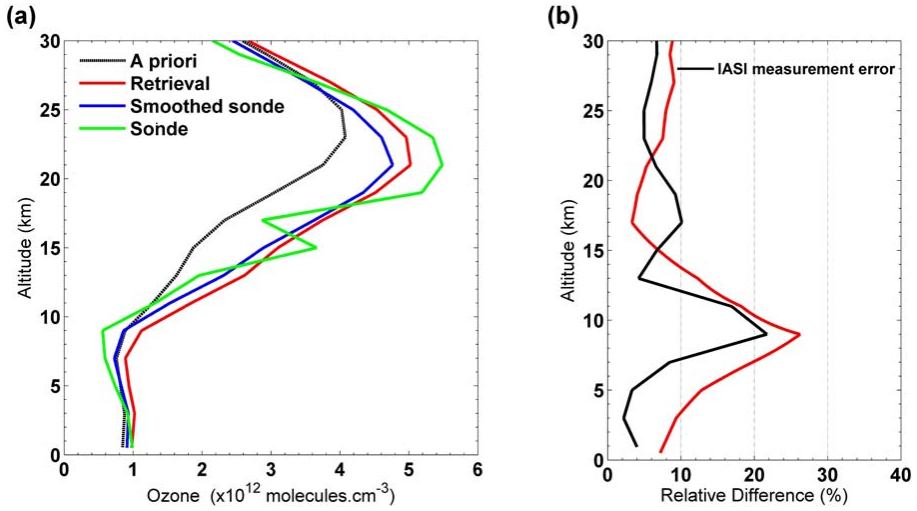

Fig. 11. **(a)** Example of retrieved ozone profile from a IASI observation made on 9 January 2008 at Legionowo station in Germany, with the sonde profile measured at this station (before and after smoothing). **(b)** Relative differences (red) calculated with respect to the smoothed sonde profile. The IASI measurement error (black) is also shown.

ACPD
9, 10513–10548, 2009

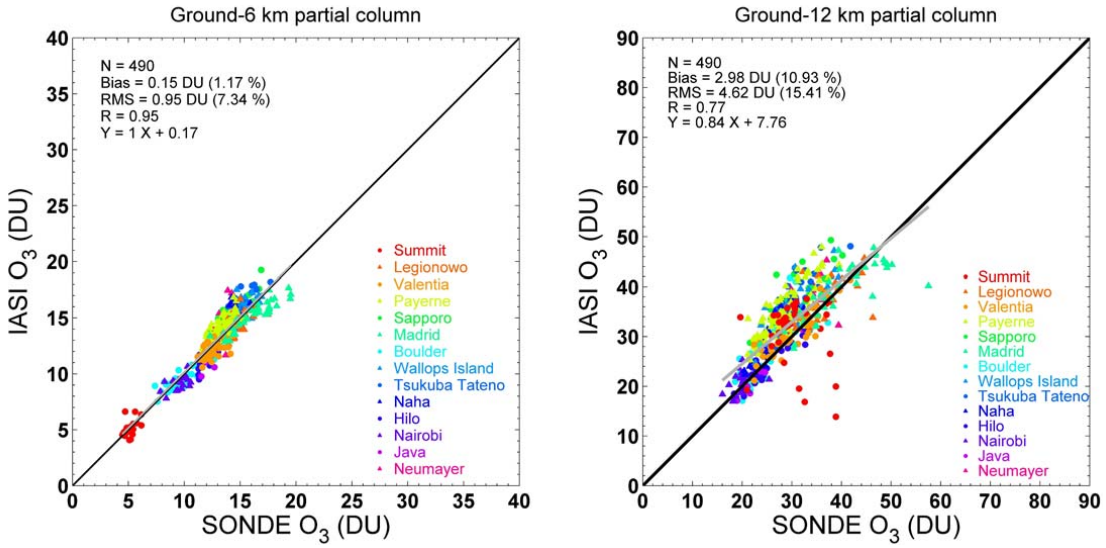

Fig. 12. Scatter plots of the IASI and sonde tropospheric ozone columns for the June 2007–August 2008 period. The shaded line represents the linear regressions between all data points and the black line, of unity slope, is shown for reference. The bias (in relative value) is calculated according to: 100*(IASI-SONDE)/SONDE.

ACPD
9, 10513–10548, 2009